

## ENCIT-2018-0012

# ESTIMATION OF AERODYNAMIC WARMING OF SPACE VEHICLES WITH NON-ZERO ANGLE OF ATTACK

**Caio Victor Lima da Silva**

**Cláudia Regina de Andrade**

Instituto Tecnológico de Aeronáutica – ITA, São José dos Campos, Brazil

[caio.vlsilva@gmail.com](mailto:caio.vlsilva@gmail.com)

[claudia@ita.br](mailto:claudia@ita.br)

**Humberto Araujo Machado**

Instituto de Aeronáutica e Espaço – IAE, São José dos Campos, Brazil

Universidade do Estado do Rio de Janeiro – UERJ, Faculdade de Tecnologia – FAT. Resende, Brazil

[humbertoham@fab.mil.br](mailto:humbertoham@fab.mil.br)

***Abstract.** Space vehicles are subject to intense warming when crossing the atmosphere. The heat must be prevented from penetrating the ship's systems and cargo in a way that does not impair its mission. Such protection is provided by a heat shield which, in order to be well designed and dimensioned, requires the engineers to know the conditions to which the vehicle is subjected. For the preliminary design, simple calculations provide a good north for this forecast, and a simple and fast model to execute can save project resources while providing a good estimate for the initial cycle of the project. The present study aims to apply and validate an analytical model that provides a good estimation of the surface flow of the SARA vehicle at specific points of its trajectory and within a typical range of angles of attack for the re-entry of the same, allied to a low computational and temporal cost. The analytical model is compared with numerical results to verify the accuracy of the estimative and evaluate its performance in diverse cases.*

***Keywords:** Aerodynamic warming, Space Vehicles, Non-zero angle of attack.*

## 1. INTRODUCTION

Aerodynamic heating is a consequence of the hypersonic flight within the atmosphere, i.e., below 100 km of altitude. Depending on the velocity and trajectory, the air temperature around the nose top may surpass 2000° C at the stagnation point. In such a situation aerodynamic heating plays a very important role in the vehicle design. Besides the effects of high temperatures on the mechanical behaviour of the structure and on-board devices, it is mandatory to preserve the payload, by using an efficient TPS (Thermal Protection System). TPS design demands an accurate estimation of the heat flux in the vehicle wall. In the preliminary stages of design, approximate analytical methods are more suitable, since the costs for numerical simulation or prototype tests are high. Zoby's Method (Zoby, 1981) is the most accepted and used procedure to perform such estimations. However, this method is only applicable in axisymmetric bodies with zero angle of attack. In this work, a modified form of Zoby's Method is tested in the SARA sub-orbital platform in a reentry trajectory with a non-zero angle of attack.

The SARA Sub-orbital Platform. Fig.1, is planned as a recoverable platform for experiments in microgravity environment, and is being developed by the Institute of Aeronautics and Space (IAE) in São José dos Campos. It has a total weight of 250 kg and a payload of 25 kg. The orbital version will be able to perform microgravity experiments and keep in an orbit of 300 km during 10 days (Moraes, 1998). SARA trajectory characteristics are showed in Fig.2.

## 2. METHODOLOGY

To predict the heat transfer on SARA, it is necessary to know pressure, temperature and velocity fields around the rocket. The Zoby's Method is used and the following simplifying assumptions are made (Miranda and Mayall, 2001):

- Vehicle rotation around its longitudinal axis is neglected;
- Atmospheric air is considered to behave as a calorically and thermally perfect gas (no chemical reactions);
- The free stream conditions ahead of the nose cap are those given by  $v_\infty$ ,  $T_\infty$ ,  $p_\infty$ , corresponding, respectively, to velocity, temperature and pressure;
- The current lines near the body walls are assumed to pass through the normal portion of the shock wave formed ahead of the nose.

By knowing  $v_\infty$  and altitude, as function of time, together with an ISA atmospheric model, it is possible to evaluate the free stream properties, such as  $p_\infty$ ,  $T_\infty$ , and  $c_\infty$ , which represent free stream pressure, temperature and speed of sound, respectively. For supersonic flow ( $M_\infty > 1$ ), a detached shock wave appears ahead of the nose. By using the normal shock relationships, it is possible to calculate  $v$ ,  $T$  and  $p$  after the shock. In the first case, the heat flux over the external surface was calculated through the Zoby's method considering zero angle of attack.

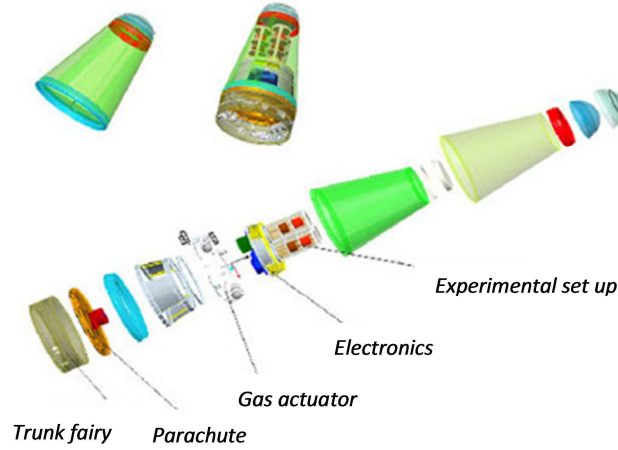


Figure 1. SARA Sub-orbital Platform.

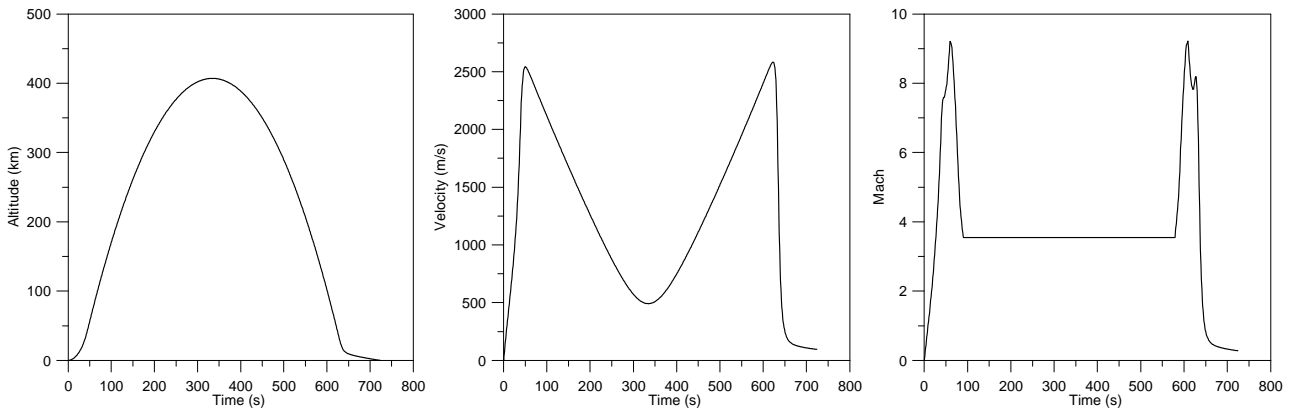


Figure 2. Trajectory of SARA sub-orbital.

The heat flux over the external surface was calculated through:

$$q = H(T_{aw} - T_w) \quad (1)$$

where  $q$  is heat flux,  $T_w$  is the wall temperature and  $T_{aw}$  is the adiabatic wall temperature, also called recovery temperature,  $T_r$ , given by:

$$T_{aw} = T_e + F_R \frac{v_e^2}{2c_p} \quad (2)$$

where  $c_p$  is the specific heat,  $T_e$  the temperature and  $v_e$  the velocity. The subscript  $e$  refers to conditions at the boundary layer edge.  $F_R$  is the recovery factor, equal to  $\sqrt{Pr_w}$ , for laminar flow and  $\sqrt[3]{Pr_w}$  for turbulent flow.  $Pr_w$  is the Prandtl number evaluated at wall temperature,  $Pr_w = 0.71$ . The convective heat transfer coefficient comes from the Reynolds analogy, namely:

$$H = 0.5\rho_e c_p v_e Pr_w^{-a} C_F \quad (3)$$

where  $a$  is equal to 0.6 for laminar flow and 0.4 for turbulent flow. To take into account compressibility effects, a modified friction factor is obtained:

$$C_F = K_1 (Re_\theta)^{K_2} \left( \frac{\rho_e^*}{\rho_e} \right) \left( \frac{\mu_e^*}{\mu_e} \right)^{K_3} \quad (4)$$

In the equation above,  $Re_\theta$  is the Reynolds number, based on the boundary layer thickness,  $\theta$

$$Re_\theta = \frac{\rho_e V_e \theta}{\mu_e} \quad (5)$$

The superscript “\*” refers to properties evaluated at Eckert’s reference temperature ( $T_e^*$ ). Viscosity,  $\mu$ , is evaluated according to Sutherland’s equation, as function of temperature and  $\rho$  is the specific mass. In Eq.(4)  $K_1 = 0.44$ ,  $K_2 = -1$  and  $K_3 = 1$ , for laminar flow. For turbulent flow,  $K_2 = K_3 = -m$ , and

$$K_1 = 2 \left( \frac{1}{C_5} \right)^{\frac{2N}{N+1}} \left[ \frac{N}{(N+1)(N+2)} \right]^m \quad (6.a)$$

$$m = \frac{2}{N+1} \quad (6.b)$$

$$C_5 = 2.2433 + 0.93N \quad (6.c)$$

$$N = 12.76 - 6.5 \log_{10}(Re_\theta) + 1.21 [\log_{10}(Re_\theta)]^2 \quad (6.a)$$

For laminar flow, the boundary layer thickness is given by:

$$\theta_L = \frac{0.664 \left( \int_0^y \rho_e^* \mu_e^* v_e R^2 dy \right)^{\frac{1}{2}}}{\rho_e v_e R} \quad (7)$$

where  $y$  is measured along the body’s surface and  $y=0$  corresponds to the stagnation point, and  $R$  is a geometric parameter schematically shown in Fig.(3), where the curved red line represents the nose cap surface.

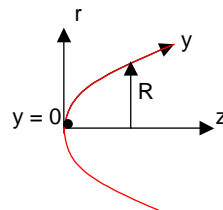


Figure 3. Coordinate system.

In this work the numerical integration of Eq. (7) was obtained according to the trapezoidal method. As  $R \rightarrow 0$ , Eq. (7) becomes undetermined. By taking the limit of Eq. (7) as  $R \rightarrow 0$ , the following expression is obtained:

$$\theta_L = \frac{0.332 (\rho_e^* \mu_e^*)^{\frac{1}{2}}}{\rho_e \sqrt{\frac{1}{R_N} \left[ \frac{2(p_s - p_\infty)}{\rho_s} \right]^{\frac{1}{2}}}} \quad (8)$$

Eq. (8) is applied for  $y < 0.1 R_N$ , where  $R_N$  is the radius of curvature at the stagnation point.

The boundary layer thickness for turbulent flow is obtained by solving the following first order differential equation:

$$\frac{D(\rho_e v_e R \theta_T)}{Dy} = 0.5 C_{fT} \rho_e v_e R \quad (9)$$

After obtaining the boundary layer momentum thickness,  $\theta$ ,  $Re_\theta$ ,  $C_F$  and  $H$  can be evaluated by using Eqs. (5), (4) and (3), respectively. Along the transition region between laminar and turbulent flow, the following relationship is used<sup>11</sup>:

$$q_{Tr} = q_L + F(y)(q_T - q_L) \quad (10)$$

where the subscripts  $Tr$ ,  $L$  and  $T$  represent, respectively, transitional, laminar and turbulent flow. The transitional factor,  $F(y)$ , is given by:

$$F(y) = 1 - \exp\left\{-0.412 \left[ \frac{4.74(y - y_L)}{(y_T - y_L)} \right]\right\} \quad (11)$$

Transition is supposed to occur for  $163 < Re_\theta < 275$ .

Properties evaluation at the boundary layer edge is performed assuming isentropic flow between the stagnation region and the location “ $i$ ” where properties are needed, namely

$$\rho_{e,i} = \rho_s \left( \frac{p_{e,i}}{p_s} \right)^{\frac{1}{\gamma}} ; h_{e,i} = h_s \left( \frac{p_{e,i}}{p_s} \right)^{\frac{\gamma-1}{\gamma}} ; v_{e,i} = \sqrt{2(h_s - h_{e,i})} ; T_{e,i} = \frac{h_{e,i}}{c_p} \quad (12)$$

The local pressure,  $p_{e,i}$ , is obtained from the modified Newton’s method and  $\gamma=1.4$ . The subscript “ $s$ ” appearing in Eqs.(12) refers to the stagnation condition. Eckert’s reference temperature is obtained from (Anderson, 1989):

$$\frac{T_{e,i}^*}{T_{e,i}} = 1 + 0.032 M_{e,i}^2 + 0.58 \left( \frac{T_w}{T_{e,i}} - 1 \right) \quad (13)$$

The solution procedure can be summarized as follows:

- i. From a given trajectory the US Standard Atmosphere (NOA, 1976) is used to obtain the free stream properties, including the stagnation ones;
- ii. Normal shock relationships are used to obtain the fluid flow properties behind the shock;
- iii. By using the modified Newton method, pressure distribution is obtained along the payload;
- iv. Equations (12) provide the local properties at the boundary layer edge;
- v. If  $y < 0.1 R_N$ , Eq. (8) provides the laminar boundary layer thickness, leading to the estimation of  $Re_\theta$ ,  $C_F$  and  $H$ , provided by Eqs. (5), (4) and (3), respectively;
- vi. If  $y > 0.1 R_N$  and  $Re_\theta < 163$ , Eq. (7) is numerically integrated up to the location where the momentum thickness is to be estimated. Such an integration is performed by using the trapezoidal method;
- vii. If  $y > 0.1 R_N$  and  $Re_\theta > 275$ , Eq. (9) is numerically integrated by the trapezoidal rule leading to the turbulent boundary layer thickness;
- viii. If  $y > 0.1 R_N$  and  $163 < Re_\theta < 275$ , Eqs. (10) and (11) are used to estimate  $H$ ;

It should be pointed out that such a procedure is performed along the payload’s surface (following the  $y$ -coordinate), for different trajectory times. Therefore,  $H=H(y,t)$ .

During a real flight, the vehicle assumes diverse angles of attack. In this case, the problem is no longer considered to be axisymmetric and the method fails in estimate the heat flux. As a solution a correction is proposed: an expansion represented by a truncated series is used to calculate the friction coefficient according with the angle of attack  $\alpha$ :

$$C_D = C_{D,0} + 12(1 - C_{D,0})\text{sen}^2\left(\frac{\alpha}{2}\right) - 6(6 - 5C_{D,0})\text{sen}^4\left(\frac{\alpha}{2}\right) + 4(6 - 5C_{D,0})\text{sen}^6\left(\frac{\alpha}{2}\right) \quad (14)$$

Where  $C_{D,0}$  is the drag coefficient for zero angle of attack calculated in the previous way. The new expression for  $C_{D,0}$  is replaced in the equation for estimation of the heat transfer coefficient, Eq.(3) (Silva, 2017).

### 3. RESULTS

Diverse points of SARA trajectory were analyzed through the approximation, with and without angle of attack. A model was generated and a numerical simulation was performed through the software ANSYS Fluent, Figs.(4-6) and the results obtained through both methods were compared. In Figures (7-9), results for  $0^\circ$ ,  $5^\circ$  and  $10^\circ$  angles of attack show a good agreement between the approximation and the software, respectively. The peak of heat flux was well estimated, although the point where it occurs presents a small discrepancy.

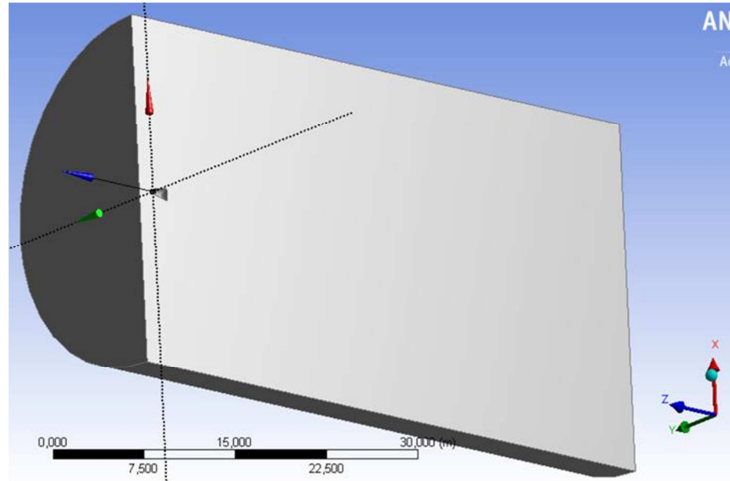


Figure 4. Domain of calculation used in ANSYS Fluent.

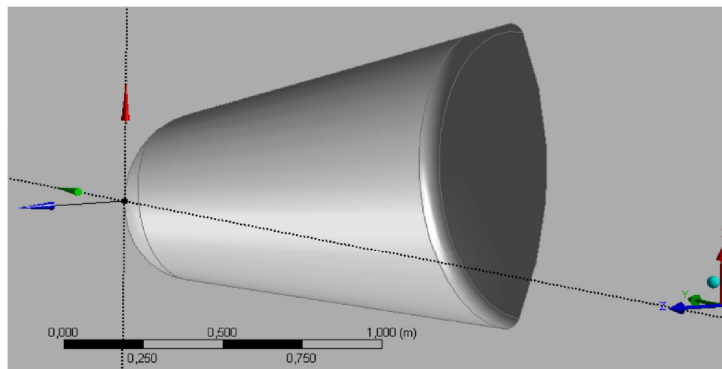


Figure 5. Model used in ANSYS Fluent.

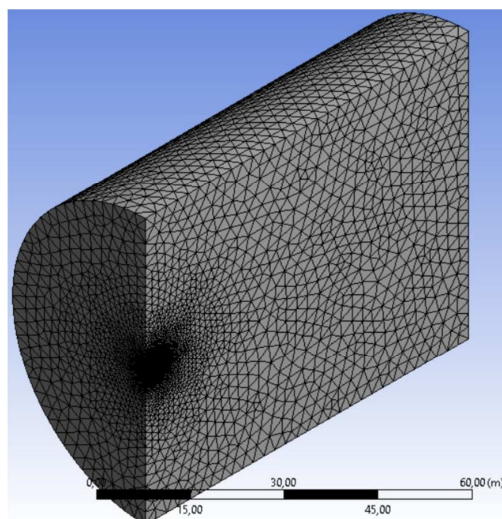


Figure 6. Mesh generated for simulation in ANSYS Fluent.

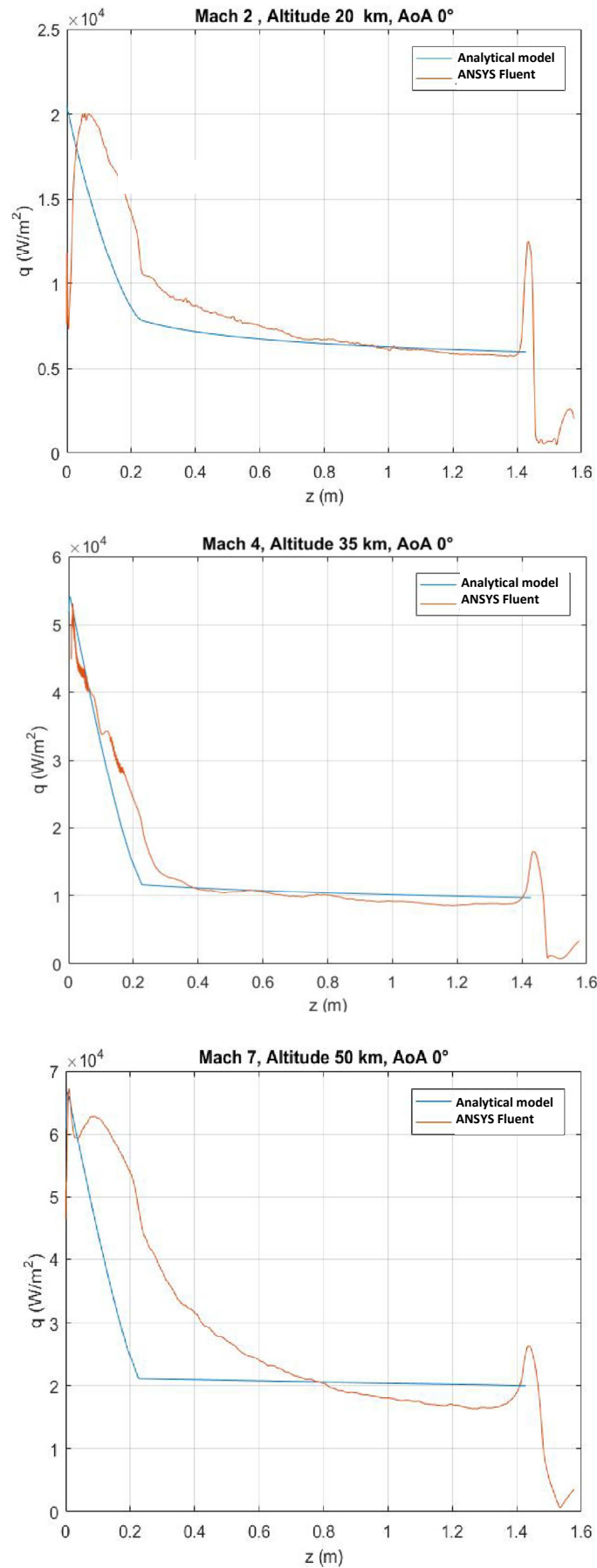


Figure 7. Results for  $0^\circ$  angle of attack.

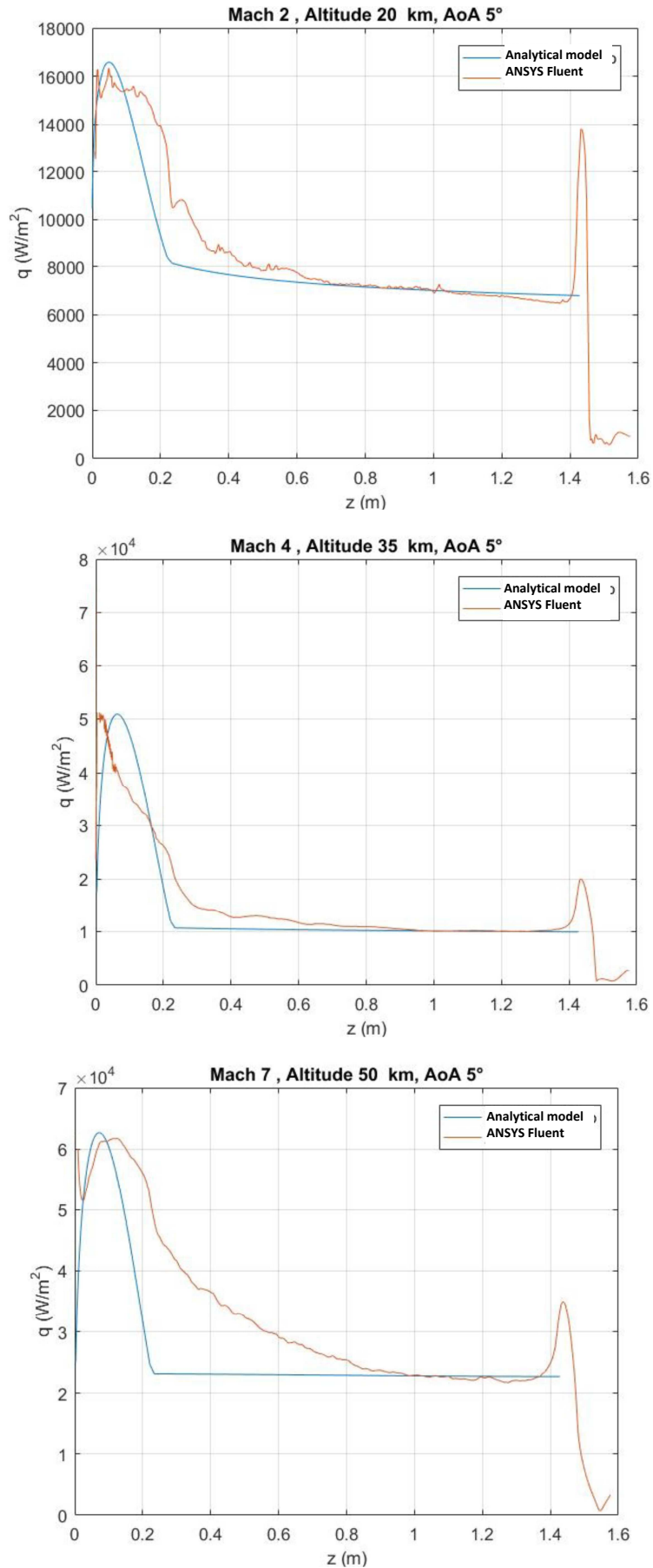


Figure 8. Results for 5° angle of attack.

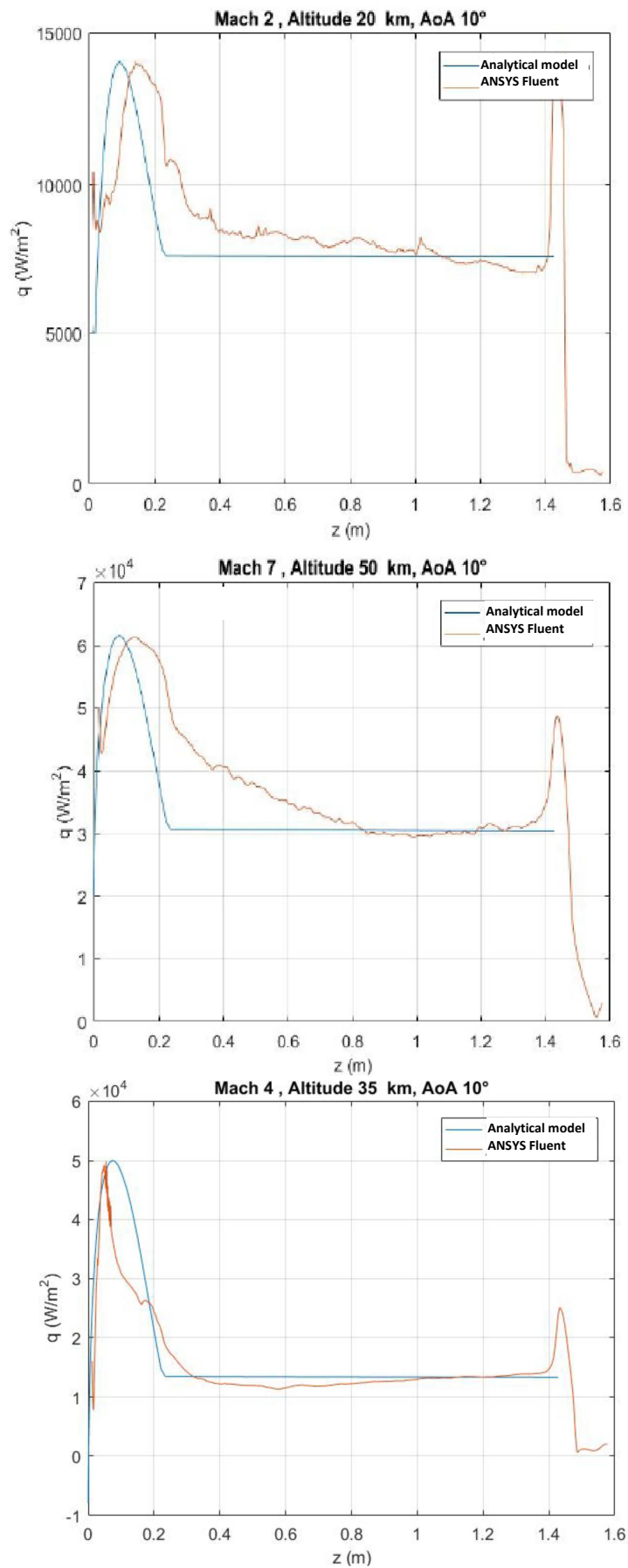


Figure 9. Results for 10° angle of attack.

According with the results, the comparison among the analytical model and CFD simulation presents good agreement when the curve behavior and order of magnitude is compared. However, analytical curves are quite smooth when compared with the oscillating CFD ones. The curve peaks are well reproduced in both, position and value, in most of the cases.

#### **4. CONCLUSIONS**

In this work, a correction for the Zoby's Method to estimate heat flux due aerodynamic warming in axisymmetric bodies at non-zero angle of attack was compared to CFD simulations for diverse Mach numbers and angles of attack.

A comparison with a 3D numerical simulation with the ANSYS Fluent presented good agreement. Some discrepancies were observed in the transition region from the spherical to the conical sections. However, the method was considered suitable for the initial phases of a vehicle design.

#### **5. REFERENCES**

- Miranda, I. F.; Mayall, M. C. M., 2001, "Fluxo de Calor Convectivo em Microssatélites em Reentrada Atmosférica", Trabalho de Conclusão de Curso (Engenharia Aeronáutica), ITA, São José dos Campos.
- Moraes Jr., P., 1998, "Design Aspects of the Recoverable Orbital Platform SARA", Proceedings of 8th Chilean Congress of Mechanical Engineering, Concepción, Chile.
- National Oceanic and Atmospheric Administration - NOAA, 1976, "U.S. Standard Atmosphere", U.S. Government Printing Office, Washington, D.C., USA.
- Silva, C. V. L., 2017, "Estimativa de Aquecimento Aerodinâmico de Veículos Orbitais e Sub-Orbitais com Ângulo de Ataque Não-Nulo", Trabalho de Graduação, ITA, São José dos Campos, SP.
- Zoby, E.; Moss, J.; Sutton, K., 1981, "Approximate convective heating equations for hypersonic flows", Journal of Spacecraft and Rockets, Vol. 18, n. 1, pp. 64-70.

#### **6. RESPONSIBILITY NOTICE**

The authors are the only responsible for the printed material included in this paper.